

# Robust joint reconstruction of misaligned images using semi-parametric dictionaries

---

Gilles Puy<sup>1,2</sup>

Pierre Vandergheynst<sup>1</sup>

<sup>1</sup>Institute of Electrical Engineering, EPFL, CH-1015 Lausanne

<sup>2</sup>Institute of the Physics of Biological Systems, EPFL, CH-1015 Lausanne, Switzerland

ICML, Edinburgh, June 2012

---

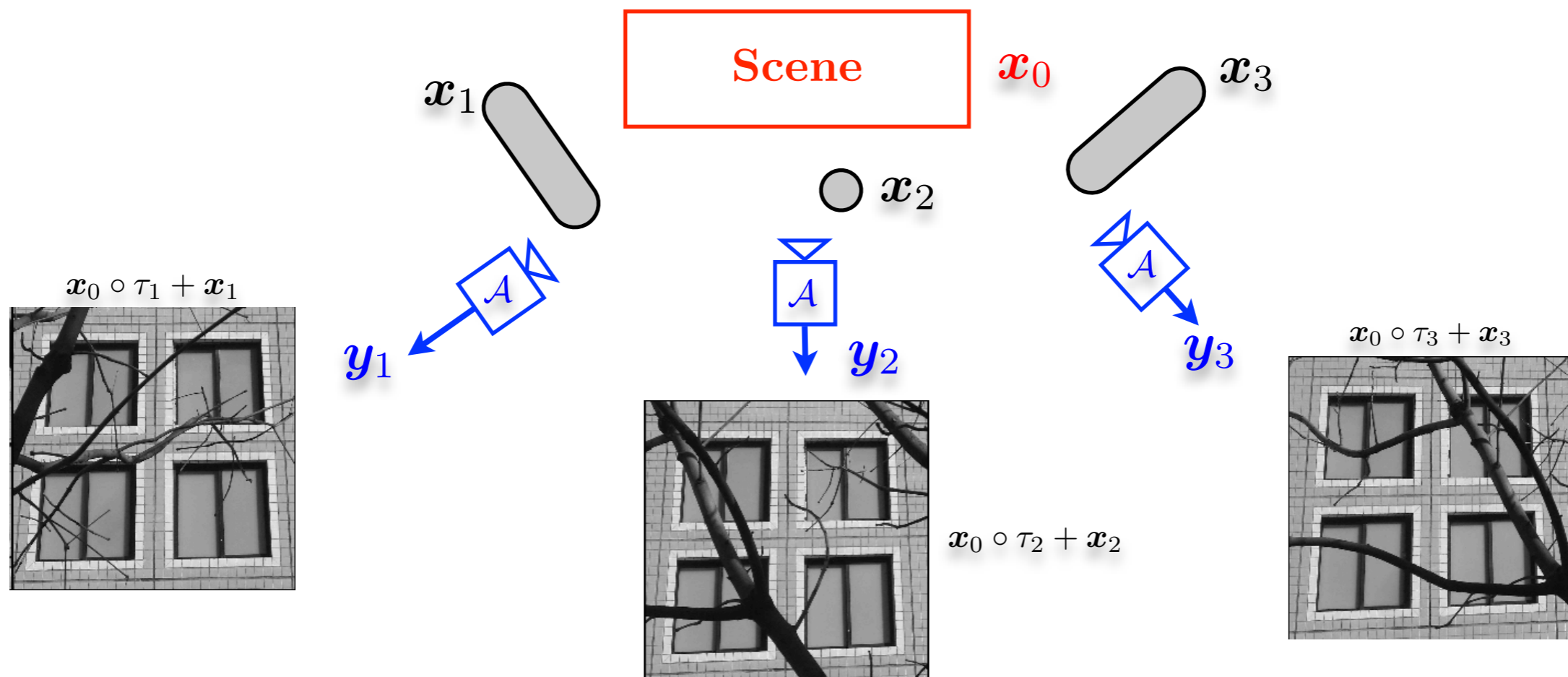


---

- I -  
Motivation

# Motivation

- A scene  $x_0$  is observed from different point of views, providing  $l$  noisy measurement vectors  $y_1, \dots, y_l \in \mathbb{R}^m$ .
- The observation system is modeled by a linear operator  $A$ .
- This scene undergoes geometric transformations  $\tau_1, \dots, \tau_l$  that depend on the position of the observer.
- The scene is partly occluded by some objects  $x_1, \dots, x_l$ .



---

- II -

# Problem formulation

# Problem formulation

---

- We discretize the images on a square grid of  $\sqrt{n} \times \sqrt{n}$  pixels,  $n \geq m$ :  $\mathbf{x}_0, \dots, \mathbf{x}_l \in \mathbb{R}^n$ .
- The linear operator  $\mathcal{A}$  is represented by  $\mathbf{A} \in \mathbb{R}^{m \times n}$ .
- The transformations  $\tau_1, \dots, \tau_l$  belong to a transformation group represented by  $p$  parameters  $\theta_j \in \mathbb{R}^p, \forall j \in \{1, \dots, l\}$ .
- The transformed image  $x_0 \circ \tau_j$  on the discrete grid is obtained by applying  $S(\theta_j)$  to  $\mathbf{x}_0$  (e.g., bilinear or bicubic spline interpolation).
- The observation model reads as

$$\underbrace{\begin{bmatrix} \mathbf{y}_1 \\ \vdots \\ \mathbf{y}_l \end{bmatrix}}_{\mathbf{y}} = \begin{bmatrix} \mathbf{A}S(\theta_1) & \mathbf{A} & \dots & \mathbf{0} \\ \vdots & \vdots & \ddots & \vdots \\ \mathbf{A}S(\theta_l) & \mathbf{0} & \dots & \mathbf{A} \end{bmatrix} \underbrace{\begin{bmatrix} \mathbf{x}_0 \\ \vdots \\ \mathbf{x}_l \end{bmatrix}}_{\mathbf{x}} + \begin{bmatrix} \mathbf{n}_1 \\ \vdots \\ \mathbf{n}_l \end{bmatrix}.$$

# Problem formulation

---

- The inverse ill-posed problem is regularized by assuming that the scene  $\mathbf{x}_0$  and the occluding objects  $\mathbf{x}_1, \dots, \mathbf{x}_l$  are sparse in a wavelet basis  $W \in \mathbb{R}^{n \times n}$ .
- The decomposition of  $\mathbf{x}_j$  in  $W$  is denoted  $\boldsymbol{\alpha}_j \in \mathbb{R}^{n \times n}$ ,  $1 \leq j \leq l$ .
- We want to solve the following non-convex problem:

$$\min_{\boldsymbol{\alpha}, \theta} \|\boldsymbol{\alpha}\|_1 + \kappa \|\mathbf{A}(\theta) \boldsymbol{\alpha} - \mathbf{y}\|_2^2 \quad \text{s.t.} \quad \theta \in \mathcal{T},$$

?

$$\text{with } \boldsymbol{\alpha} = [\boldsymbol{\alpha}_0, \dots, \boldsymbol{\alpha}_l]^T \text{ and } \mathbf{A}(\theta) = \begin{bmatrix} \mathbf{A}S(\theta_1)W & \mathbf{A}W & \dots & 0 \\ \vdots & \vdots & \ddots & \vdots \\ \mathbf{A}S(\theta_l)W & 0 & \dots & \mathbf{A}W \end{bmatrix}.$$

# Problem formulation

- The inverse ill-posed problem is regularized by assuming that the scene  $\mathbf{x}_0$  and the occluding objects  $\mathbf{x}_1, \dots, \mathbf{x}_l$  are sparse in a wavelet basis  $W \in \mathbb{R}^{n \times n}$ .
- The decomposition of  $\mathbf{x}_j$  in  $W$  is denoted  $\boldsymbol{\alpha}_j \in \mathbb{R}^{n \times n}$ ,  $1 \leq j \leq l$ .
- We want to solve the following non-convex problem:

$$\min_{\boldsymbol{\alpha}, \mathbf{z}, \theta} \|\boldsymbol{\alpha}\|_1 + \underbrace{\kappa}_{\text{Large}} \|\mathbf{A}(\theta) \boldsymbol{\alpha} - \mathbf{z}\|_2^2 \quad \text{s.t.} \quad \begin{cases} \|\mathbf{y}_1 - \mathbf{z}_1\|_2 \leq \epsilon_1 \\ \vdots \\ \|\mathbf{y}_l - \mathbf{z}_l\|_2 \leq \epsilon_l \end{cases} \quad \text{and } \theta \in \mathcal{T},$$

$$\text{with } \boldsymbol{\alpha} = [\boldsymbol{\alpha}_0, \dots, \boldsymbol{\alpha}_l]^\top, \quad \mathbf{A}(\theta) = \begin{bmatrix} \mathbf{A}\mathbf{S}(\theta_1)\mathbf{W} & \mathbf{A}\mathbf{W} & \dots & 0 \\ \vdots & \vdots & \ddots & \vdots \\ \mathbf{A}\mathbf{S}(\theta_l)\mathbf{W} & 0 & \dots & \mathbf{A}\mathbf{W} \end{bmatrix},$$

$$\text{and } \mathbf{z} = [\mathbf{z}_0, \dots, \mathbf{z}_l]^\top.$$

---

- III -  
Method



# Method

---

- Objective function:  $\mathcal{L}(\boldsymbol{\alpha}, \mathbf{z}, \theta) = \|\boldsymbol{\alpha}\|_1 + \kappa \|\mathbf{A}(\theta) \boldsymbol{\alpha} - \mathbf{z}\|_2^2 + i_{\mathcal{B}(\mathbf{y}, \epsilon)}(\mathbf{z}) + i_{\mathcal{T}}(\theta)$ .

Indicator functions of the sets  $\mathcal{B}(\mathbf{y}, \epsilon) = \{\mathbf{z} = \{z_j\}_{1 \leq j \leq l} : \|\mathbf{y}_j - z_j\|_2 \leq \epsilon_j\}$  and  $\mathcal{T}$ .

- Solve this non-convex problem using a proximal method (Attouch et al.):

- Initializations: set  $k = 0$ ,  $\boldsymbol{\alpha}^0 = \mathbf{0} \in \mathbb{R}^{(l+1)n}$ ,  $\mathbf{z}^0 = \mathbf{y}$ ,  $\theta^0 \in \mathcal{T}$ , choose  $0 < \lambda_{\min} \leq \lambda_{\mathbf{z}}, \lambda_{\theta}$ ,  $\{\lambda_{\boldsymbol{\alpha}}^k\}_{k \in \mathbb{N}} \leq \lambda_{\max}$  and  $b > 0$ .

- Repeat:

1)  $(\boldsymbol{\alpha}^{k+1}, \mathbf{z}^{k+1}) \in \underset{\boldsymbol{\alpha}, \mathbf{z}}{\operatorname{argmin}} \mathcal{L}(\boldsymbol{\alpha}, \mathbf{z}, \theta^k) + \lambda_{\mathbf{z}} \|\mathbf{z} - \mathbf{z}^k\|_2^2 + \lambda_{\boldsymbol{\alpha}}^k \|\boldsymbol{\alpha} - \boldsymbol{\alpha}^k\|_2^2$ .

2) Find  $\theta^{k+1} \in \mathcal{T}$  such that:

$$\kappa \|\mathbf{A}(\theta^{k+1}) \boldsymbol{\alpha}^{k+1} - \mathbf{z}^{k+1}\|_2^2 + \lambda_{\theta} \|\theta^{k+1} - \theta^k\|_2^2 \leq \kappa \|\mathbf{A}(\theta^k) \boldsymbol{\alpha}^{k+1} - \mathbf{z}^{k+1}\|_2^2,$$

$$\|\nabla_{\theta} \mathcal{L}(\boldsymbol{\alpha}^{k+1}, \mathbf{z}^{k+1}, \theta^{k+1})\|_2^2 \leq b \|\theta^{k+1} - \theta^k\|_2^2.$$

3)  $k \leftarrow k + 1$ .

- Under some mild conditions, the algorithm converges to a critical point of  $\mathcal{L}$ .

# Method

- Objective function:  $\mathcal{L}(\boldsymbol{\alpha}, \mathbf{z}, \theta) = \|\boldsymbol{\alpha}\|_1 + \kappa \|\mathbf{A}(\theta) \boldsymbol{\alpha} - \mathbf{z}\|_2^2 + i_{\mathcal{B}(\mathbf{y}, \epsilon)}(\mathbf{z}) + i_{\mathcal{T}}(\theta)$ .

Indicator functions of the sets  $\mathcal{B}(\mathbf{y}, \epsilon) = \{\mathbf{z} = \{z_j\}_{1 \leq j \leq l} : \|\mathbf{y}_j - z_j\|_2 \leq \epsilon_j\}$  and  $\mathcal{T}$ .

- Solve this non convex-problem using a proximal method (Attouch et al.):

- Initializations: set  $k = 0$ ,  $\boldsymbol{\alpha}^0 = \mathbf{0} \in \mathbb{R}^{(l+1)n}$ ,  $\mathbf{z}^0 = \mathbf{y}$ ,  $\theta^0 \in \mathcal{T}$ , choose  $0 < \lambda_{\min} \leq \lambda_{\mathbf{z}}, \lambda_{\theta}$ ,  $\{\lambda_{\boldsymbol{\alpha}}^k\}_{k \in \mathbb{N}} \leq \lambda_{\max}$  and  $b > 0$ .

- Repeat:

1)  $(\boldsymbol{\alpha}^{k+1}, \mathbf{z}^{k+1}) \in \underset{\boldsymbol{\alpha}, \mathbf{z}}{\operatorname{argmin}} \mathcal{L}(\boldsymbol{\alpha}, \mathbf{z}, \theta^k) + \lambda_{\mathbf{z}} \|\mathbf{z} - \mathbf{z}^k\|_2^2 + \lambda_{\boldsymbol{\alpha}}^k \|\boldsymbol{\alpha} - \boldsymbol{\alpha}^k\|_1$ .

2) Find  $\theta^{k+1} \in \mathcal{T}$  such that:

$$\kappa \|\mathbf{A}(\theta^{k+1}) \boldsymbol{\alpha}^{k+1} - \mathbf{z}^{k+1}\|_2^2 + \lambda_{\theta} \|\theta^{k+1} - \theta^k\|_2^2 \leq \kappa \|\mathbf{A}(\theta^k) \boldsymbol{\alpha}^{k+1} - \mathbf{z}^{k+1}\|_2^2,$$

$$\|\nabla_{\theta} \mathcal{L}(\boldsymbol{\alpha}^{k+1}, \mathbf{z}^{k+1}, \theta^{k+1})\|_2^2 \leq b \|\theta^{k+1} - \theta^k\|_2^2.$$

3)  $k \leftarrow k + 1$ .

until *convergence*.

# Method

---

- By construction  $\mathcal{L}$  is not increasing. Indeed,  $k \geq 0$ ,

$$\mathcal{L}(\alpha^{k+1}, z^{k+1}, \theta^{k+1}) + \lambda_z \|z^{k+1} - z^k\|_2^2 + \lambda_\theta \|\theta^{k+1} - \theta^k\|_2^2 + \lambda_\alpha^k \|\alpha^{k+1} - \alpha^k\|_1 \leq \mathcal{L}(\alpha^k, z^k, \theta^k).$$

- We also have:

$$\sum_{k=0}^{+\infty} \|z^{k+1} - z^k\|_2^2 + \|\theta^{k+1} - \theta^k\|_2^2 + \|\alpha^{k+1} - \alpha^k\|_1 < +\infty.$$

- Convergence to a critical point of  $\mathcal{L}$  ?

---

- IV -

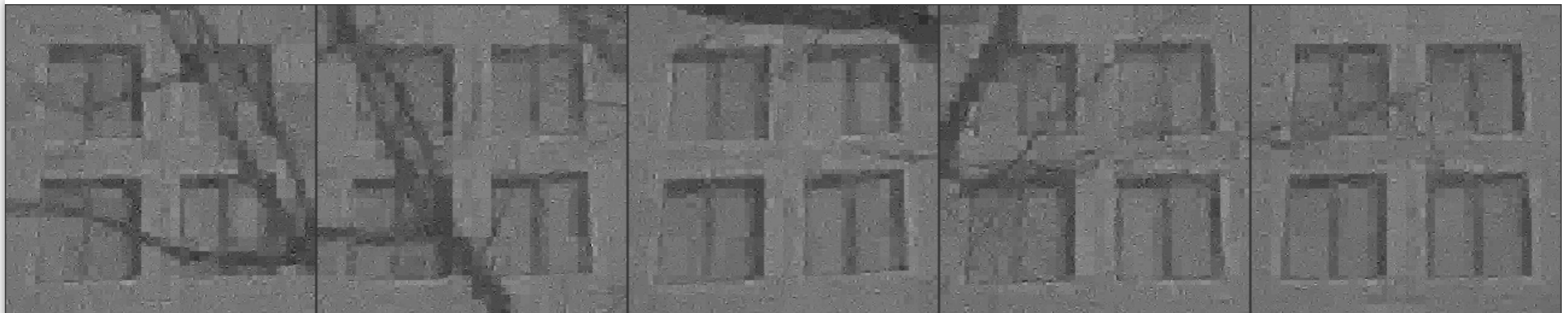
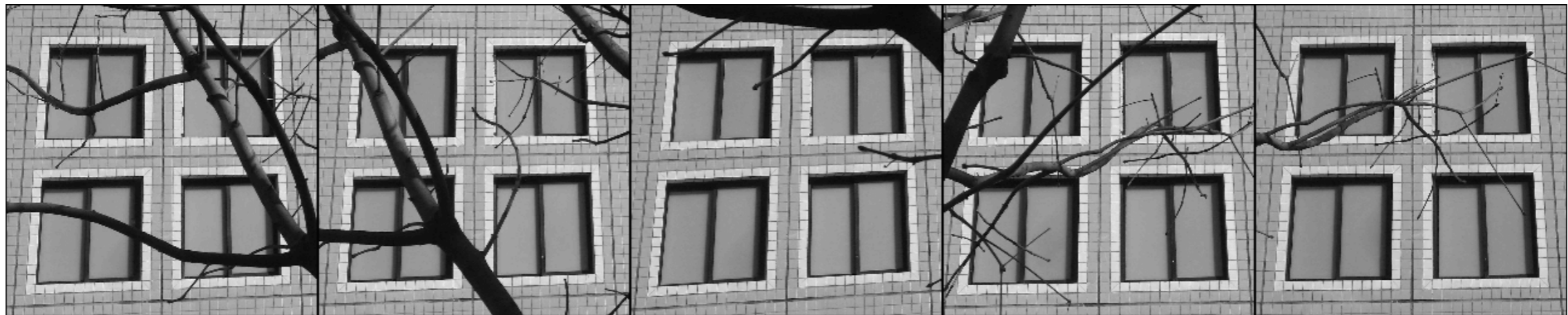
# Simulation results

# Simulations results

---

- $m = 0.1n$  measurements per image obtained with the spread spectrum technique [6].
- The transformations are assumed to be homographies modeled by 8 unknown parameters.

Original images



Solving the Basis Pursuit independently for each image

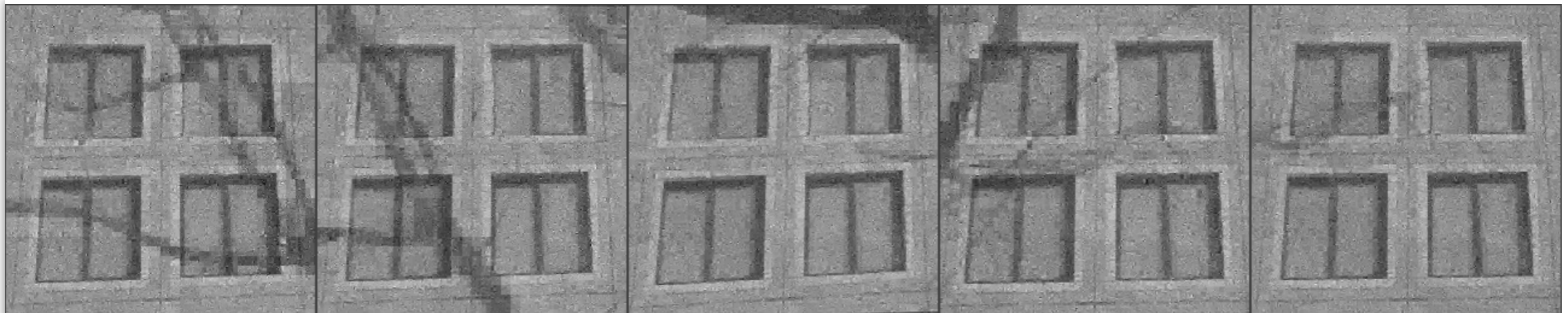
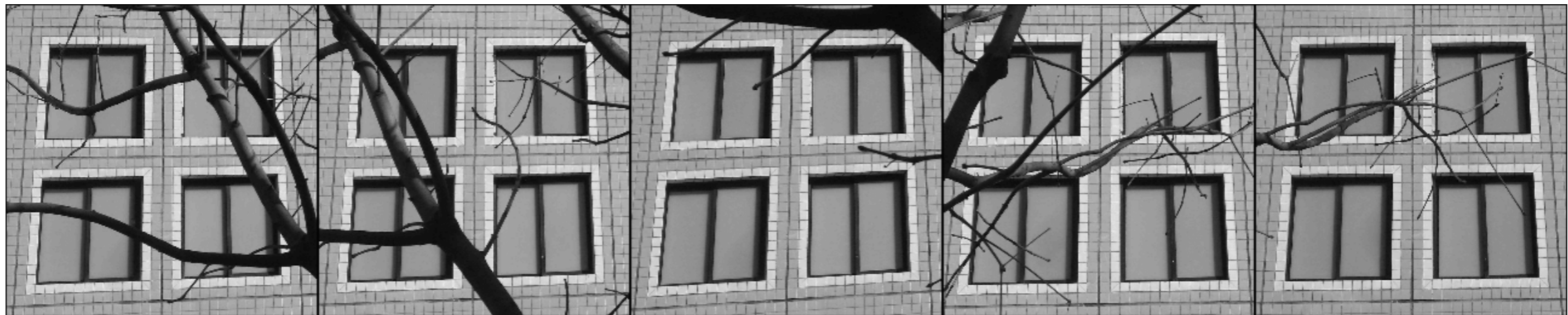


# Simulations results

---

- $m = 0.1n$  measurements per image obtained with the spread spectrum technique [6].
- The transformations are assumed to be homographies modeled by 8 unknown parameters.

Original images



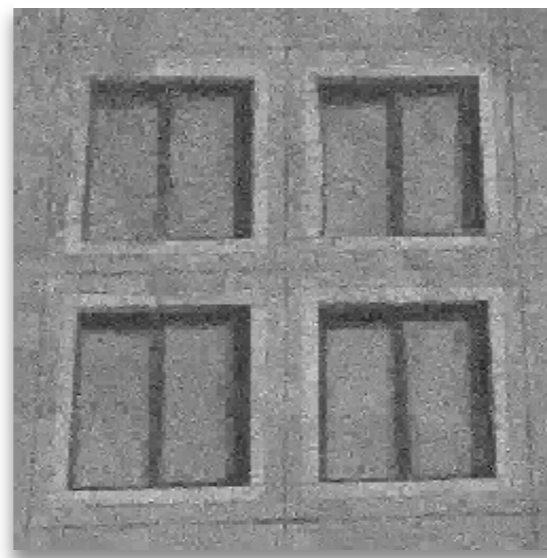
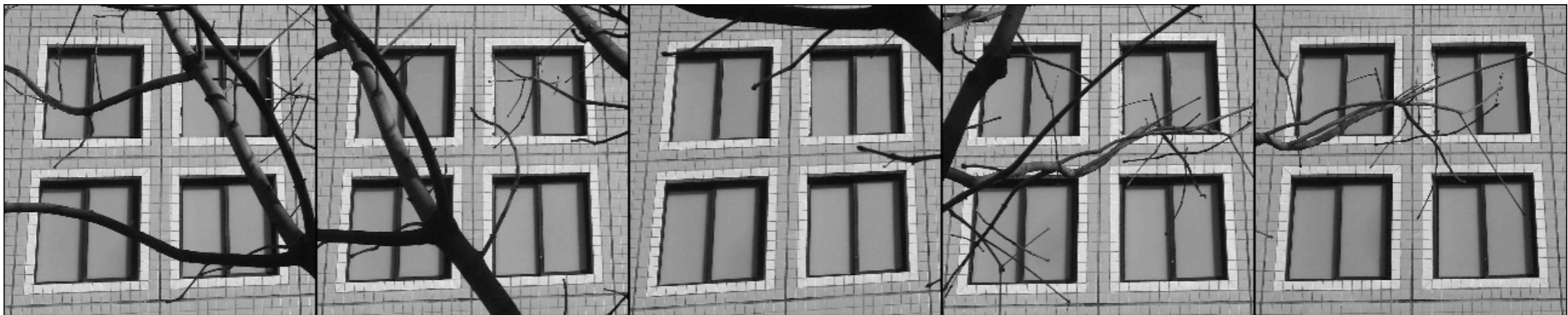
Reconstruction with the proposed method

# Simulations results

---

- $m = 0.1n$  measurements per image obtained with the spread spectrum technique [6].
- The transformations are assumed to be homographies modeled by 8 unknown parameters.

Original images



Background image

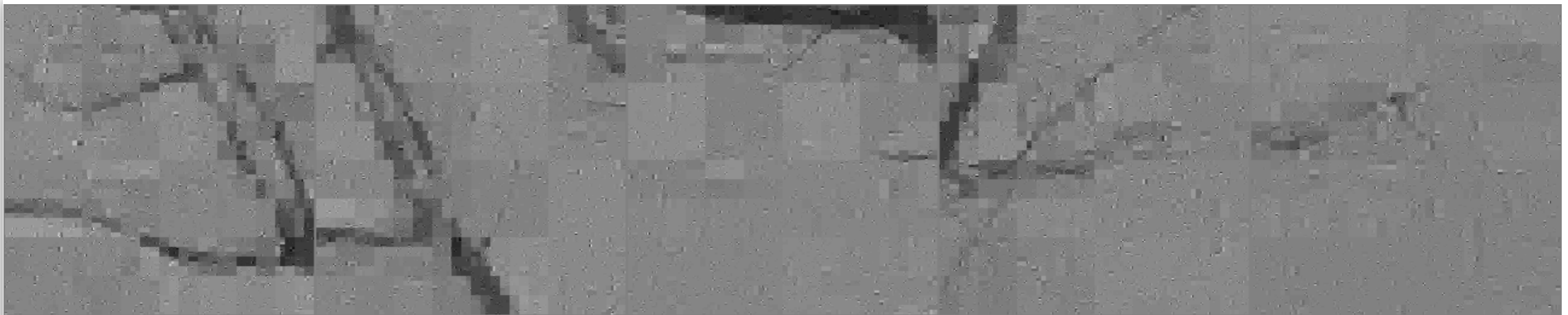
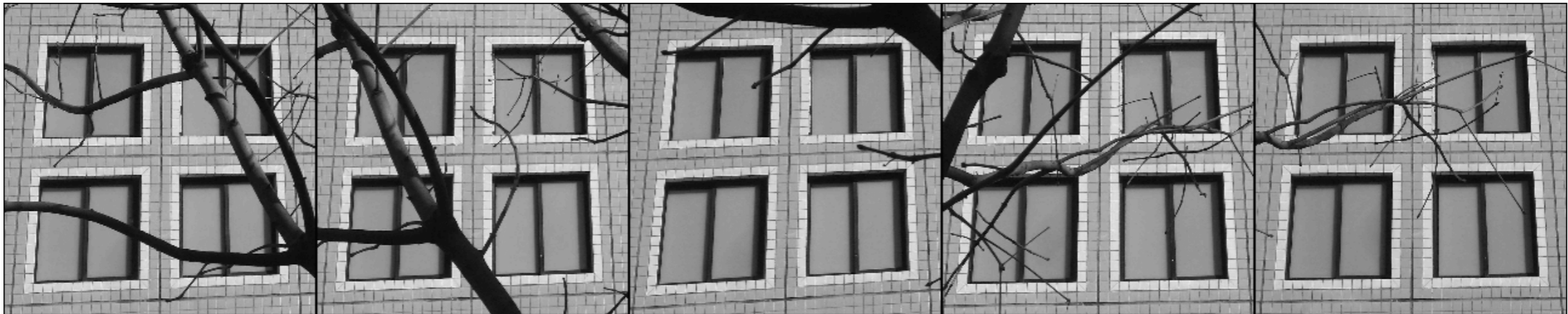


# Simulations results

---

- $m = 0.1n$  measurements per image obtained with the spread spectrum technique [6].
- The transformations are assumed to be homographies modeled by 8 unknown parameters.

Original images



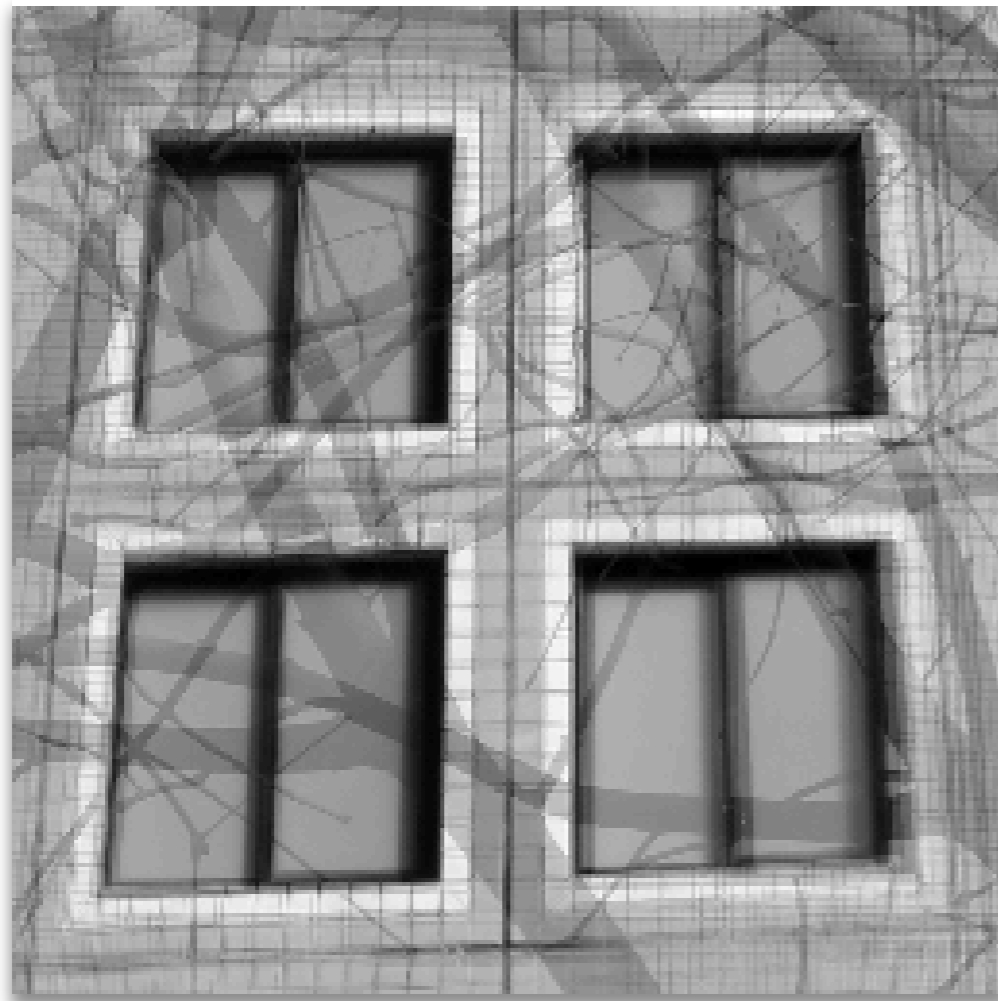
Foreground images



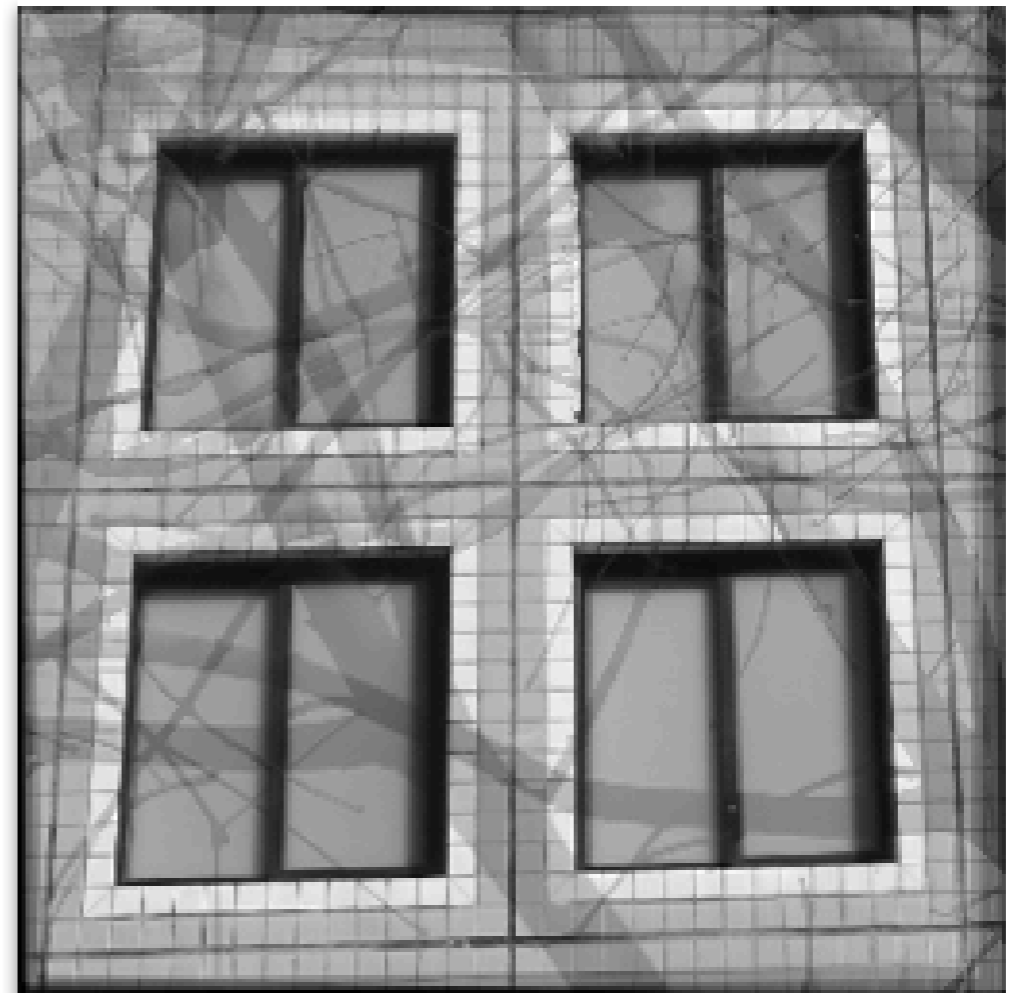
# Simulations results

---

- $m = 0.1n$  measurements per image obtained with the spread spectrum technique [6].
- The transformations are assumed to be homographies modeled by 8 unknown parameters.



Superposed unregistered images.

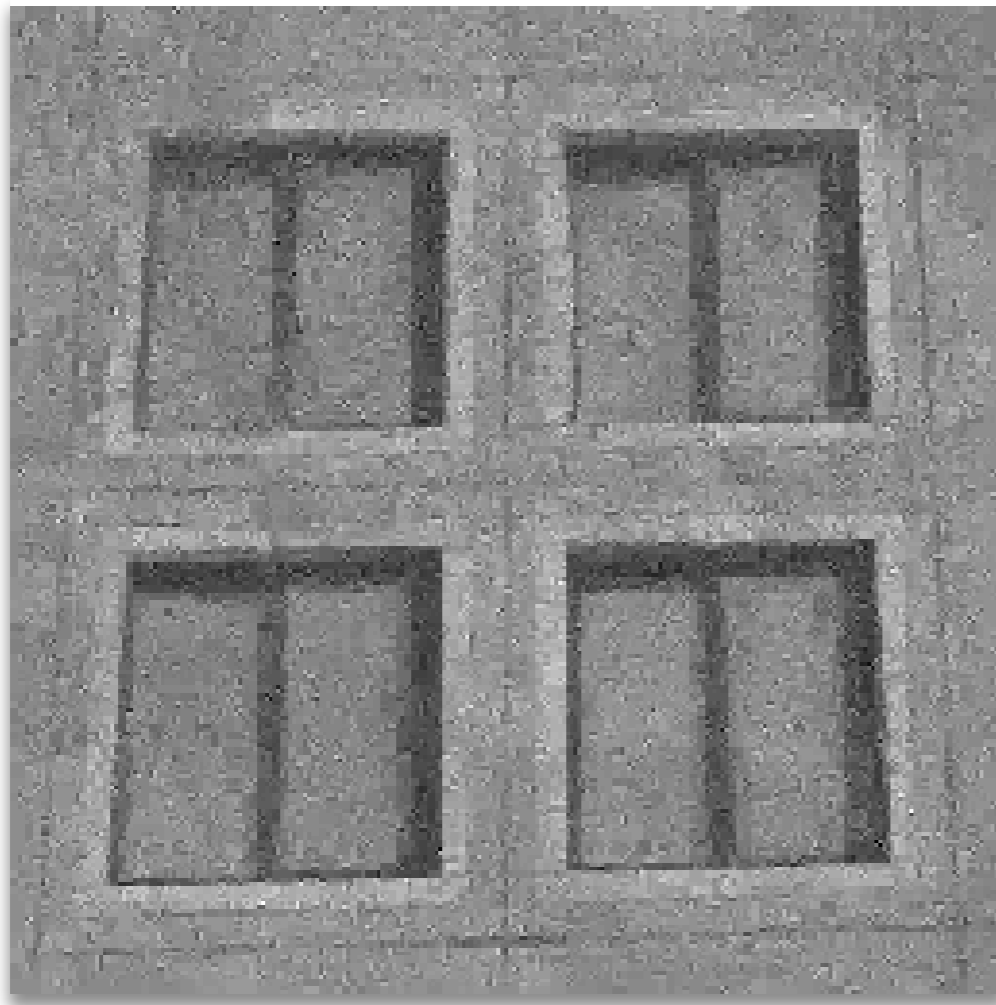


Superposed registered images.

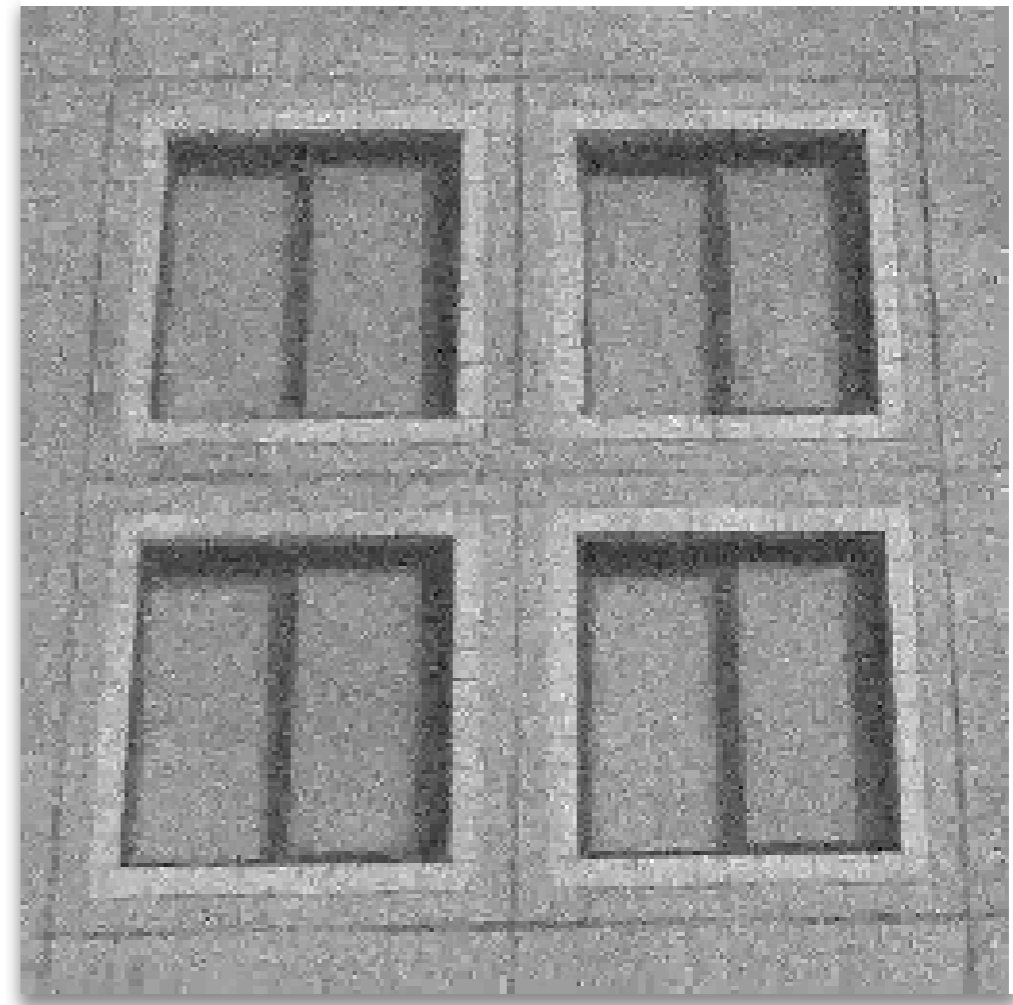
# Simulations results

---

- $m = 0.1n$  measurements per image obtained with the spread spectrum technique [6].
- The transformations are assumed to be homographies modeled by 8 unknown parameters.



Estimated background image with  
5 measurements vectors



Estimated background image with  
10 measurements vectors

# Simulations results

- Repeat the experiments for different number of measurements and noise levels on the following 5 images:



Castle-R20 dataset available at [cvlab.epfl.ch](http://cvlab.epfl.ch) (Strecha et al., CVPR, 2008).

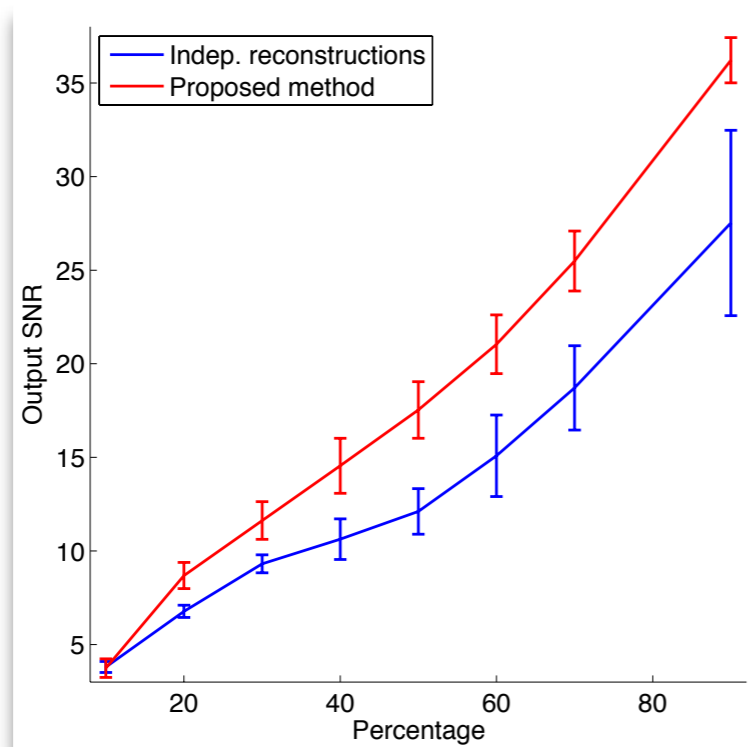


Image quality vs. Nb. measurements

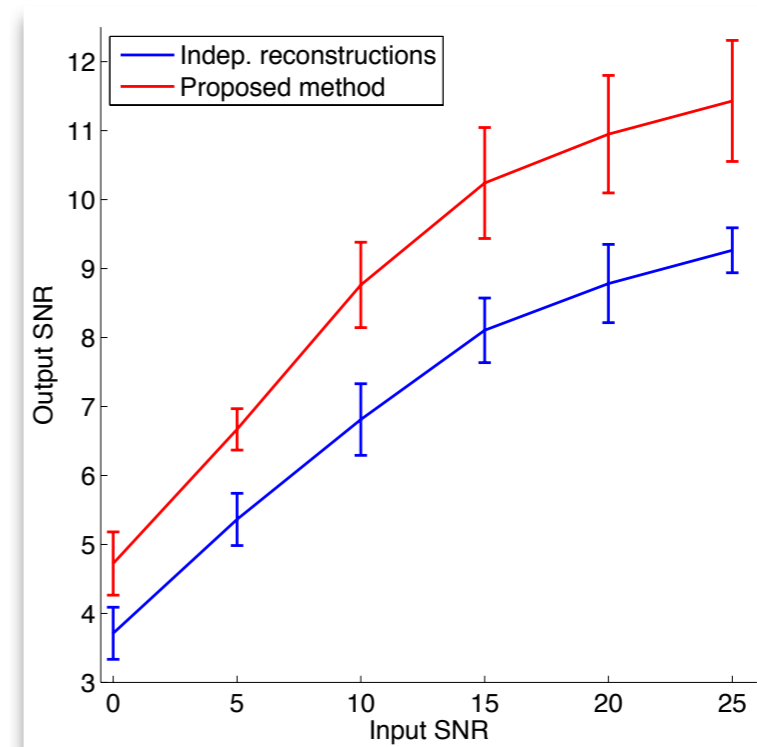


Image quality vs. Noise level

# Simulations results

---

- Repeat the experiments for different number of measurements and noise levels on the following 5 images:

From 30% of measurements



Superposed unregistered images.



Superposed registered images.

---

- V -

# Conclusion & Perspectives

# Conclusion & Perspectives

---

- We proposed a method for compressed multi-view imaging that:
  - unifies the reconstruction and the registration in the same setting.
  - is robust to occlusions and noise measurements.
  - separates automatically the background image from the foreground images (occlusions)
- Application to free breathing coronary MRI or magnetic resonance spectroscopic imaging.